JOURNAL OF AGRICULTURAL AND FOOD CHEMISTRY

ARTICLE

pubs.acs.org/JAFC

Gene Cloning, Expression, and Characterization of a Nitrilase from *Alcaligenes faecalis* ZJUTB10†

Zhi-Qiang Liu,[‡,§] Li-Zhu Dong,[‡,§] Feng Cheng,[‡,§] Ya-Ping Xue,[‡,§] Yuan-Shan Wang,[‡,§] Jie-Nv Ding,[‡,§] Yu-Guo Zheng,[*,‡,§] and Yin-Chu Shen[‡,§]

[‡]Institute of Bioengineering, Zhejiang University of Technology, Hangzhou 310014, People's Republic of China

[§]Engineering Research Center of Bioconversion and Biopurification, Ministry of Education, Zhejiang University of Technology, Hangzhou 310014, People's Republic of China

ABSTRACT: Nitrilases are important industrial enzymes that convert nitriles directly into the corresponding carboxylic acids. In the current work, the fragment with a length of 1068 bp that encodes the *A. faecalis* ZJUTB10 nitrilase was obtained. Moreover, a catalytic triad was proposed and verified by site-directed mutagenesis, and the detailed mechanism of this nitrilase was clarified. The substrate specificity study demonstrated that the *A. faecalis* ZJUTB10 nitrilase belongs to the family of arylacetonitrilases. The optimum pH and temperature for the purified nitrilase was 7−8 and 40 °C, respectively. Mg^{2+} stimulated hydrolytic activity, whereas Cu^{2+}, Co^{2+}, Ni^{2+}, Ag^{+}, and Hg^{2+} showed a strong inhibitory effect. The K_m and v_{max} for mandelonitrile were 4.74 mM and 15.85 μmol min^{-1} mg^{-1} protein, respectively. After 30 min reaction using the nitrilase, mandelonitrile at the concentration of 20 mM was completely hydrolyzed and the enantiomeric excess against (*R*)-(−)-mandelic acid was >99%. Characteristics investigation indicates that this nitrilase is promising in catalysis applications.

KEYWORDS: Nitrilase, *Alcaligenes faecalis*, structure modeling, characterization, enantioselective hydrolysis

INTRODUCTION

Recently, environmental concerns are rising because of waste accumulation and limited supplies of petroleum feedstocks, which has resulted in a higher demand for advanced enzymatic or green approaches to perform efficient chemical reactions.[1] Several enzymes have been exploited to perform stereo- and regioselective chemical transformations to prepare kinds of molecules useful for applications in the foodstuff, pharmaceutical, and chemical industries.[2,3]

Nitrilase (EC 3.5.5.1), as an important industrial enzyme, is a valuable biocatalyst that hydrolyzes nonpeptide carbon−nitrogen bonds. Nitrilase belongs to the nitrilase family of CN-hydrolyzing enzymes,[4] which has drawn substantial interest as a valuable alternative to chemical hydrolysis in organic chemical processes and detoxification of cyanide wastes.[5−7] In addition, recently nitrilase has been widely used in the preparation of pharmaceutical intermediates and phytocides and in the textile industry.[8,9] Nitrilases are preferred over chemical methods because they can convert nitriles directly into the corresponding carboxylic acids in a single step, are often used under ambient conditions, and do not result in large amounts of byproducts.[10] Nitrilase has the remarkable ability to readily facilitate chemical hydrolysis processes and thus represents an excellent tool to perform detailed structure−activity analysis. Studies on nitrilases have been widely carried out in terms of their occurrences, applicabilities, catalytic mechanisms, and cloning of the nitrilase genes from different origins.[11−13] On the basis of the substrate specificity, nitrilases are classified into three major categories including aromatic nitrilases, aliphatic nitrilases, and arylacetonitrilases, making them useful for the hydrolysis of a large number of nitriles.[14] Nitrilases have been found in many plants and microorganisms.[15] A variety of nitriles have been transformed by different kinds of nitrilases.[14] Recently, screening new nitrilases and exploring new applications are becoming popular research activities.

In our previous work, a strain of *Alcaligenes faecalis* ZJUTB10 with a high nitrilase activity toward the conversion of racemic mandelonitrile to (*R*)-(−)-mandelic acid was isolated and characterized. The nitrilase specific activity reached 350.8 U/g and the highest production rate was 9.3 mmol h^{-1} g^{-1}.[16] From its high enzymatic activity and tolerance to a high concentration of products, this strain appears promising for potential applications in industry to produce carboxylic acids from nitriles.[16]

The objectives of the research were to clone and express the gene encoding nitrilase from *A. faecalis* ZJUTB10 as well as perform an investigation of characteristics for purified nitrilase and a prediction of the three-dimensional (3D) structure model based on sequence similarity. These primary features suggest that the *A. faecalis* nitrilase is a suitable enzyme for degradation or modification of nitriles by the biocatalysis route.

MATERIALS AND METHODS

Bacterial Strains, Plasmids, and Culture Conditions. *A. faecalis* ZJUTB10, grown in a medium that consisted of ammonium acetate 12.14 g/L, yeast extract 7.79 g/L, K_2HPO_4, 5 g/L, $MgSO_4$ 0.2 g/L, NaCl 1 g/L, and *n*-butyronitrile 3.29 g/L, pH 7.5, has been deposited at the China Center for Type Culture Collection (CCTCC M 208168, Wuhan, China).[16] The *Escherichia coli* strains JM109 (Tiangen biotech Co., Ltd., Beijing, China) and BL21 (DE3) (Invitrogen, Karlsruhe,

Received: July 9, 2011
Accepted: September 13, 2011
Revised: August 31, 2011
Published: September 13, 2011

Germany) were used as hosts for cloning and expression experiments, respectively. The plasmids pMD18-T (TaKaRa, Otsu, Japan) and pET-28b(+) (Novagen, Darmstadt, Germany), carrying an N-terminal and a C-terminal 6×His-Tag sequence, were used for cloning and expression of nitrilase, respectively. *E. coli* and recombinant *E. coli* strains were grown in Luria−Bertani (LB) (yeast extract 5 g/L, tryptone 10 g/L, NaCl 5 g/L) liquid medium at 37 °C. To maintain the presence of the plasmids, ampicillin and kanamycin were added to the media for *E. coli* harboring plasmids pMD18-T and pET28b(+), respectively.

Gene Manipulation. DNA manipulation, plasmid isolation, and agarose gel electrophoresis were conducted according to standard protocol [17] unless stated otherwise.

Construction of pMD18-NIT Cloning Vector. The genomic DNA of *A. faecalis* ZJUTB10 was used as the template, and the open reading frame of the nitrilase gene was amplified by PCR. The primers that were designed based on the reported amino acid sequences of nitrilases in NCBI (Accession Nos. P20960 and CAC09069) for the amplification of genes NIT were P1: 5′-ATGCAGACTCGTAAA-ATTGTT-3′ and P2: 5′- GGACGGTTCCTGAACCAG-3′. The PCR reaction mixture consisted of 20 ng of genomic DNA, 50 μM for each dNTP, 0.5 μM P1 and P2, 5 μL of 10×*Pfu* DNA buffer, and 2 U *Pfu* DNA polymerase (Biocolor, Shanghai, China) in 50 μL. PCR was carried out in 50 μL using a Thermocycler (Bio-Rad, Hercules, CA). PCR products were visualized on a 1.5% ethidium bromide stained gel. The reaction was carried out at 94 °C for 5 min, followed by 35 cycles at 94 °C for 45 s, 55 °C for 45 s for amplifying the nitrilase gene, 72 °C for 2 min, and then 72 °C for 10 min in a PCR thermocycler (Bio-Rad). An approximate 1.1 kb fragment was subjected to 0.9% agarose electrophoresis and then purified (Axygen, Union City, NJ). Then the fragment was cloned into the plasmid of pMD18-T (Takara, Otsu, Japan) by T/A cloning and transformed into *E. coli* JM109 competent cells. Finally, the positive clone was sequenced. Basic Local Alignment Search Tool (BLAST, www.ncbi.nlm.nih.gov/blast) and DNAMAN Version 5.2 (Lynnon Biosoft, Quebec, Canada) were employed for the GenBank search, identity assessment, and protein domain determination. Deduced amino acid sequences were obtained from ExPASy and GenBank databases.

Construction of Expression Plasmid for Nitrilase Gene. According to the sequence of the nitrilase gene of *A. faecalis* ZJUTB10, a pair of primers was redesigned as follows: P3: 5′-AATGGATCCATG-CAGACTCGTAAAATTGTTCG-3′ and P4: 5′-AGGGTCGACG-GACGGTTCCTGAACCAGC-3′. The PCR products were double digested with *Bam*HI *and Sal*I. The resulting 1.1 kb fragments containing the intact nitrilase genes were inserted into pET28b(+) vector which had been linearized with the enzymes of *Bam*HI *and Sal*I using T4 ligase. Transformation of expression plasmids pET28b(+)-NIT into *E. coli* BL21 (DE3) was performed by the heat-shock method.

Expression and Purification of Recombinant Nitrilase. The recombinant plasmids carrying the wild type and mutant nitrilase genes were transformed into *E. coli* BL21(DE3) cells. The resulting recombinant cells were grown at 37 °C in 50 mL of LB media containing 50 μL of kanamycin (50 mg/mL). Production of enzyme was induced by addition of 0.1 mM isopropyl β-D-thiogalactoside (IPTG) when optical density at 600 nm of the culture broth reached between 0.6 and 0.8. The cells were then incubated at 28 °C for 20 h and harvested by centrifugation at 9000 rpm for 20 min. The harvested cells were washed twice with 10 mL of physiological saline solution (NaCl 0.9%). Then the cells were resuspended in 30 mL of 50 mM Tris-HCl (pH 7.5) and lysed by sonication with a Vibra-Cell VC 505 ultrasonic processor (Sonics and Materials Inc., Newtown, CT) at 350 W for 30 min. The soluble fractions of the sonified solution were obtained by centrifugation at 9000 rpm for 20 min.

The resulting crude extracts were retained for purification. The cell-free extracts were applied onto a nickel-NTA superflow column (10 mL) previously equilibrated with a binding buffer (20 mM NaH_2PO_4, pH 8.0; 300 mM NaCl). Unbound proteins were washed out from the column with a washing buffer (20 mM NaH_2PO_4, pH 8.0; 300 mM NaCl; 50 mM imidazole). Then the elution was carried out with a buffer (20 mM NaH_2PO_4, pH 8.0; 300 mM NaCl; 500 mM imidazole). The proteins were analyzed using 12% sodium dodecyl sulfate polyacrylamide gel electrophoresis (SDS-PAGE).

Construction of Nitrilase Mutants. Site-directed mutants of the nitrilase at positions of Glu-47, Lys-129, and Cys-163 were constructed using the QuickChange Site-Directed Mutagenesis Kit (Stratagene, La Jolla, CA) and pET28b(+)-NIT plasmid as a template. Glu 47 was mutated to Gln with primers Glu47Gln (F): 5′-GATCGTGTTCGGT-CAGACTTGGCTG-3′, and Glu47Gln (R): 5′-GTCTGACCGAA-CACGATCAGATCAC-3′. Lys 129 was mutated to Ile with primers Lys129Ile (F): 5′-TGTGGTCCCGTCGTATACTGAAACC-3′, and Lys129Ile (R): 5′-CAGTATACGACGGGACCACAGCATTTC-3′. Cys 163 was mutated to Gly with primers Cys163Gly (F): 5′-TGTCGGCGCTCTGTGTGGCTGGGAACATCT-3′, and Cys-163Gly (R): 5′-AGCCACACAGAGCGCCGACACGGCCCAGT-3′. Mutants were verified by sequencing, expressed, and purified in the same way as that used for the wild type enzyme.

SDS-PAGE Analysis. Crude extracts and elution fractions were analyzed by SDS-PAGE, performed using a Mini-gel system (Bio-Rad). The gels were cast with 0.75 mm spacers (Bio-Rad). Aliquots of each eluted fraction were subjected to SDS-PAGE and enzyme assay. SDS-PAGE was performed according to Laemmli's discontinuous Tris-glycine buffer system at 10 mA for 2−3 h with a 5% acrylamide stacking gel (pH 6.8) and 12% separating gel (pH 8.8).[18] Proteins in the gel were stained with Coomassie brilliant blue R-250.

Enzyme Assays and Protein Assay. The activity of nitrilase was determined by measuring the production of (*R*)-(−)-mandelic acid from mandelonitrile.[16] The standard assay was performed with mandelonitrile (20 mM) and the enzyme mixed in Tris-HCl buffer (50 mM, pH 7.5). The reaction mixture (total volume 5 mL) was incubated at 40 °C, 150 rpm. After 10 min, 500 μL of mixture was sampled, 50 μL of HCl (2 M) was added to end the reaction, and then the mixture was centrifuged at 12 000*g* for 2 min under 4 °C. The amount of mandelic acid product was determined by a LC-20AD prominence liquid chromatography instrument (Shimadzu, Kyoto, Japan) using a C18 column (5 μm × 250 nm × 4.6 nm, Elite Analytical Instruments Co., Ltd., Dalian, China) and equipped with a SPD-2A prominence UV/vis detector. Each sample (20 μL) was eluted at 30 °C with 0.01 M $(NH_4)H_2PO_4$:CH_3OH = 13:7 (v/v, 1 mL/min) as mobile phase, and A_{228} was measured.

The optical purity of (*R*)-(−)-mandelic acid was determined by analysis of the enantiomers on a CHIRALEL-OD-H column (250 × 4.6 mm) (Daicel Chemical Industries, Shinzaike, Japan) at a flow rate of 0.8 mL/min with a mobile phase containing hexane, 2-propanol, and trifluoroacetic acid (90:10:0.1, v/v) at A_{228}. Before optical purity determination, pretreatment steps were performed on the reaction mixture. The pH of the reaction mixture was adjusted to about 1.5, and then the enantiomers were extracted with equal volume of ethyl acetate. The extract obtained was concentrated, and the residual solid was dissolved in the mobile phase for HPLC determination. The ee of (*R*)-(−)-mandelic acid was calculated by the eq 1:

$$\text{ee} = [(R - S)/(R + S)] \times 100\% \quad (1)$$

where *R* and *S* represent the concentration of (*R*)-(−)-mandelic acid and (*S*)-(+)-mandelic acid, respectively.

One unit of the enzyme activity was defined as the amount of enzyme that produces 1 μmol of mandelic acid per minute under the conditions described above. Protein quantitative analysis was conducted using the Bradford method[19] with bovine serum albumin as a standard.

Table 1. Characteristics of Some Nitrilases

organism	substrate	molecular mass (kDa)	optimal pH	optimal temp (°C)	reference
Alcaligenes faecalis *Aspergillus niger* K10	mandelonitrile benzonitrile	44.2	7−8	40	this work
	4-cyanophridine	38.5	8	45	27
Geobacillus pallidus DAC521	benzonitrile				
	crotonitrile	41	7.6	65	28
Norcadia (*Rhodoccocus*) NCIMB 11216	benzonitrile				
	m-nitrobenzonitrile	45.8	8	30	29,30
Rhodococcus rhodochrous J1	benzonitrile				
	acrylonitrile	40	7.6	45	31,32
Acidovorax facilis 72W	fumaronitrile				
	benzonitrile	40	8−9	65	33,34
Bradyrhizopium japonicas USD 110(blr3397)	hydrocinnamonitrile				
	benzonitrile	34.5	7−8	45	35
Rhodococcus rhodochrous K22	acrylonitrile				
	benzonitrile	41	5.5	50	36
Alcaligenes faecalis ATCC 8750	*p*-aminobenzylcyanide				
	benzonitrile	32	7.5	45	37
Alcaligenes faecalis JM3	2-thiopheneacetonitrile				
	p-chlorobenzylcyanide	38.9	7.5	45	38,39
Bradyrhizopium japonicas USD 110(bll6402)	phenylacetonitrile				
	mandelonitrile	37	/	/	40
Pseudomonas stutzeri AK61	KCN	38	7.5	30	41
Fusarium solani	KCN, $K_2Ni(CN)_4$, $K_4Fe(CN)_6$	45	7.5	25	42

Time Course of Mandelonitrile Hydrolysis. The time course of mandelonitrile hydrolysis was examined with 20 mM mandelonitrile and the appropriate amount of enzyme under standard conditions. Samples were periodically withdrawn from separate reaction mixtures under identical conditions, and the concentrations of mandelonitrile, (*R*)-(−)-mandelic acid, and (*S*)-(+)-mandelic acid were determined.

Temperature and pH Dependence. The optimal temperature of the enzyme was determined by assaying enzyme activities at temperatures ranging from 25 °C to 65 °C. Thermostability was investigated by incubating enzymes at temperatures ranging from 35 °C to 65 °C at a final concentration of 0.1 mg/mL in 50 mM Tris-HCl buffer (pH 7.5). The incubation took place in a heat-block at the specified temperature for 1 h. The enzyme activities were assayed at 40 °C after various incubation times. To investigate the optimal pH and the effect of pH on activity of nitrilase, three different buffers with concentrations of 50 mM including potassium phosphate buffer (pH 6.0−7.5), Tris-HCl buffer (pH 7.0−9.0), and glycine−sodium hydroxide buffer (pH 8.5−10.0) were used, and reactions were performed at 40 °C using 20 mM mandelonitrile as substrate. To investigate pH stability, the enzyme was dissolved in different buffers of pHs ranging from 6.0 to 10.0 and incubated at 40 °C for 1 h, and then the relative activities were carried out in the standard enzyme assay condition. Activity without treatment obtained at pH 7.5 was used as a blank and regarded as 100%. All the experiments were performed in triplicate, and the data obtained are presented as activity without normalization.

Circular Dichorism (CD) Measurements. CD spectra were recorded on a JASCO J-815 Spectropolarimeter (JASCO Inc., Easton, MD) using Spectra Manager 228 software. The temperature was controlled using a Fisher Isotemp Model 3016S water bath (Fisher Scientific, Waltham, MA). A lyophilized powder (purity >95% w/w) was prepared. A stock solution of 0.25 mM nitrilase was generated in 20 mM sodium phosphate, pH 3.0, sodium acetate, pH 5.0, and 20 mM sodium phosphate, pH 8.0. Far-UV scans were performed at 0.15 mg/mL protein in a 10-mm cuvette. The spectra were recorded from 200 to 250 nm with a scan speed of 20 nm/min. Results are expressed in terms of mean residue ellipticity ($[\theta]_{MRW,\lambda}$) (in deg cm^2 d mol^{-1}) determined according to eq 2:[20,21]

$$[\theta]_{MRW,\lambda} = MRW(\theta_\lambda)/10lc \quad (2)$$

where MRW is the mean residue weight of the specific cutinase, θ_λ is the observed ellipticity (mdeg), l is the path length (cm), and c is the protein concentration (μM). Thermal denaturation of enzymes was followed as a function of temperature and pH by continuously monitoring ellipticity changes at 222 nm using a step size of 1 °C. Observed ellipticities were transformed to apparent fractions of denatured proteins ($f_{D,app}$) according to eq 3:

$$f_{D,app} = (\theta_T - \theta_N)/(\theta_D - \theta_N) \quad (3)$$

where θ_T is the sample ellipticity (mdeg) at a particular temperature, and θ_D and θ_N are the corresponding values for the denatured and native states, extrapolated to the same temperatures.[22] The T_m was calculated by taking the first-order derivative of the sigmodial curve obtained from the melting curve.[23] These experiments were conducted in triplicate, and averaged data are reported here.

Metal Ion and Chemical Analysis. The effects of metal ions and chemicals on the enzyme activity were measured after the enzyme was preincubated at 40 °C with various compounds at a final concentration of 5 mM for 10 min in Tris-HCl buffer at pH 7.5. After treatment, the activities were estimated according to the standard activity assay method mentioned above.

Substrate Specificity. Enzyme activity toward nitriles was determined by either the formation of ammonia or the production of carboxylic acids. The reaction was performed in a reaction mixture (0.5 mL) containing 10 mM nitrile, 50 mM pH 7.5 Tris-HCl, and an appropriate amount of the enzyme at 40 °C for 10 min with a reciprocal shaker at 150 rpm (standard conditions). The amounts of *o*-methoxyphenylacetic acid, *m*-methoxyphenylacetic acid, and *p*-methoxyphenylacetic acid were

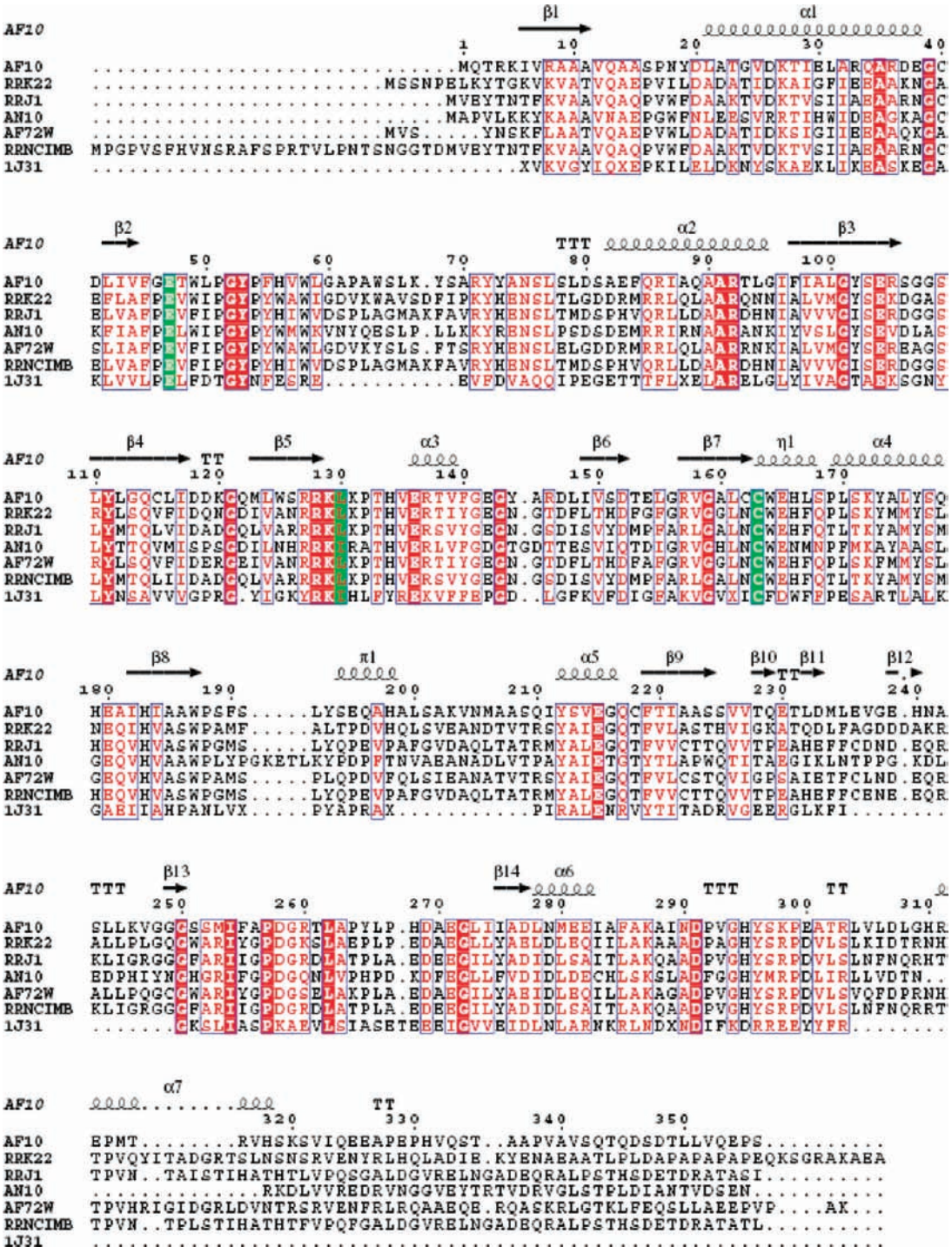

Figure 1. Structure-based alignment of nitrilase from different origins. AF10, an arylacetonitrilase nitrilase from *A. faecalis* ZJUTB10; RRK22, an aliphatic nitrilase from *Rhodococcus rhodochrous* K22 (D12583); RRJ1, an aromatic nitrilase from *R. rhodochrous* J1 (D11425); AN10, an aromatic nitrilase from *Aspergillus niger* K10 (EU282000); RRNCIMB, an aromatic nitrilase from *R. rhodochrous* NCIMB 11216 (CAC88237); 72W, an aliphatic nitrilase from *Acidovorax facilis* 72W (DQ444267); 1J31, hypothetical protein PH0642 (PDB accession code 1J31) one of the templates. The red color indicates the conserved catalytic residues: The residues influencing the triad pocket (Cys-163, Glu-47, and Lys-129) are marked in green.

determined by HPLC (LC-10AS, Shimdazu, Kyoto, Japan) using a 4.6 mm × 250 mm ODS column (Shimadazu, Kyoto, Japan). The parameters used for the detection of the compounds were a UV detector set at a wavelength of 270 nm, a flow rate of 1.0 mL/min, and a mobile phase of water/acetonitrile (50:50, v/v) containing 0.1% trifluoroacetic acid. The amounts of mandelic acid, *o*-chloromandelic acid, and phenylacetic acid were determined by a LC-20AD prominence liquid chromatography instrument (Shimadzu, Kyoto, Japan) using a C18 (5 μm × 250 nm ×4.6 nm) column (Elite Analytical Instruments Co., Ltd.) and equipped with a SPD-2A prominence UV/vis detector. Each injected sample (20 μL) was eluted at 30 °C with 10 mM $(NH_4)H_2PO_4$:CH_3OH = 13:7 (v/v, 1 mL/min) as mobile phase, and products were detected

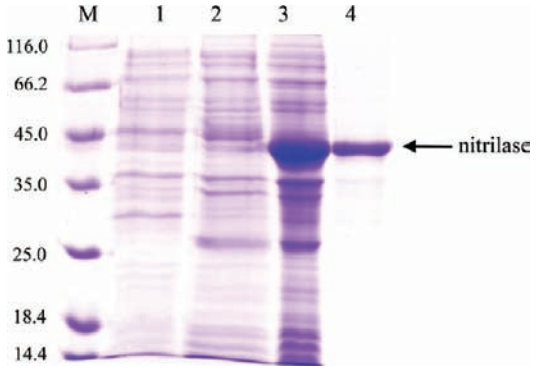

Figure 2. SDS-PAGE analysis of expression products by *E. coli* BL21-(DE3) (pET-28b(+)-NIT). Gels with 30% polyacrylamide were subjected to protein analysis, and the protein bands were stained with Coomassie blue R250. M: Protein marker β-galactosidase (116.0 kDa), bovine serum albumin (66.2 kDa), ovalbumin (45 kDa), lactate dehydrogenase (35.0 kDa), REase Bsp98I (20.1 kDa), β-lactoglobulin (18.4 kDa), and lysozyme (14.4 kDa). Lanes 1 and 2 stand for the products of *E. coli* BL21 (DE3) control and *E. coli* BL21 (DE3) [pET-28b(+)-NIT] negative, lane 3 stands for induced *E. coli* BL21 (DE3) [pET28b(+)-NIT], and lane 4 stands for purified nitrilase.

at 228 nm. A Hypersil SAX icon exchange column (Shimadazu, Kyoto, Japan) was used for quantitative analysis of iminodiacetic acid. The parameters used for the detection of the compounds were a UV detector set at a wavelength of 210 nm, a flow rate of 1.0 mL/min, and a mobile phase of 0.02 M $(NH_4)_2HPO_4$ at pH 4.0. Concentrations of 2-amino-2,3-dimethylsuccinic acid, 2,2-dimethylcyclopropanecarboxylic acid, acrylic acid, benzoic acid, acetic acid, 4-aminobenzoic acid, aminobutyric acid, and hexanedioic acid were assayed using an Agilent 6890N gas chromatograph (Agilent, Santa Clara, CA), equipped with a flame ionization detector (FID) and a FFAP column (30 m $\times$ 0.25 mm $\times$0.33 μm). The operating conditions were as follows: oven temperature was 180 °C, and the injection and detector temperature were kept at 250 °C for analysis. One unit of the enzyme activity toward each substrate was defined as the amount of enzyme required to produce 1 μmol of the corresponding acid per minute at 40 °C, respectively. The activities were given relative to the activity toward mandelonitrile. The activity toward mandelonitrile was considered as 100%.

Homology Modeling and Docking. The three-dimensional homology model of nitrilase was generated using Build Homology Models (MODELER) in Discovery Studio 2.1 (DS 2.1, Accelrys Software, San Diego, CA) using crystal structures of a hypothetical protein PH0642 (PDB accession code 1J31) and a thermoactive nitrilase (PDB accession code 3IVZ) as templates. The generated structures were improved by subsequent refinement of the loop conformations by assessing the compatibility of an amino acid sequence to known PDB structures using the Protein Health module in DS 2.1. The geometry of loop regions was corrected using Refine Loop/MODELER. Finally, the best quality model was chosen for further calculations, molecular modeling, and docking studies by Autodock 4.0.[24] Structure-based sequence alignment was performed using the program ClustalX,[25] and the picture of the sequence alignment was made using the program ESPRIPT.[26]

RESULTS

Cloning and Sequence Analysis of the Nitrilase. The products amplified with the primers P1 and P2 were subjected to agarose gel electrophoresis, and fragments of about 1.1 kb were generated. The fragments were then recovered and ligated

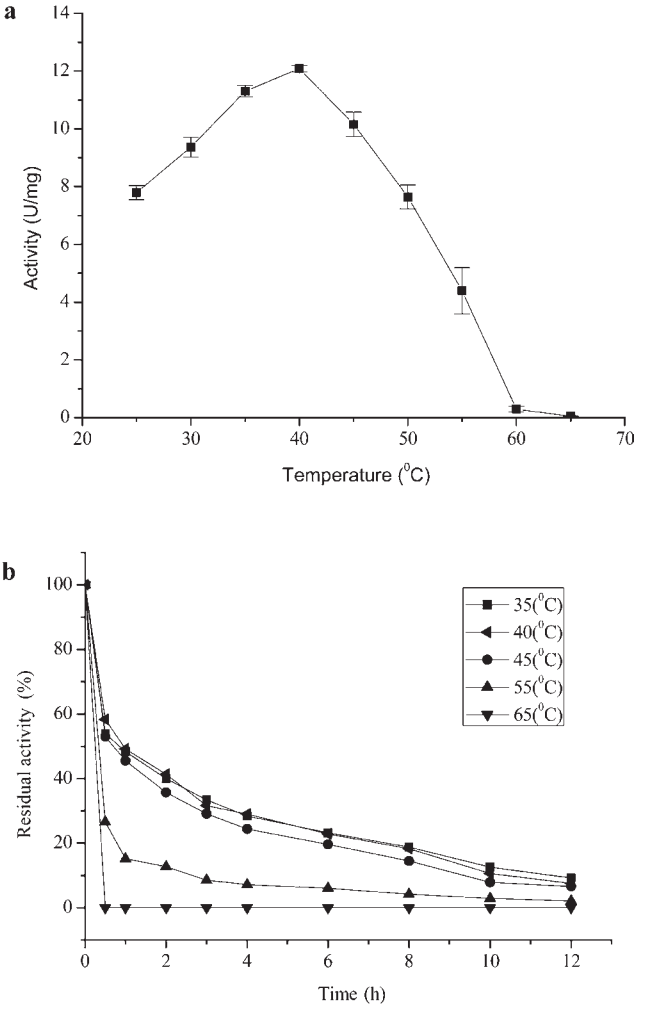

Figure 3. Effect of temperature on activity of nitrilase and stability. (a) Reactions were performed at 150 rpm for 10 min at various temperatures (25 °C to 65 °C) with 50 mM Tris-HCl buffer (pH 8.0). (b) The enzyme was preincubated at 40 °C and reacted for 10 min.

with pMD18-T, and the recombinant plasmid, named pMD18-T-NIT, was transformed into a *E. coli* JM109 competent cell by heat shock. A number of positive clones (colorless) with ampicillin resistance were obtained. Among these, three were picked to prepare the single-strand for sequence analysis. As a result, a sequence of about 1.1 kb was achieved. The sequence analysis using software DNAMAN (Version 5.2, Lynnon Biosoft, Quebec, Canada) indicated that the amplified fragment contained an ORF of 1068 bp encoding 356-amino-acid protein with a molecular mass of 41.5 kDa. The nitrilase gene sequence obtained here was submitted to the GenBank database with the accession number of HQ407378. The sequences alignment result showed that nitrilase from *A. faecalis* ZJUTB10 showed a high homology of about 78% with those of *Pseudomonas putida* strain MTCC 5110 (GeneBank acession no. EF467660) and *Alcaligenes* sp. ECU0401 (GeneBank acession no. FJ943638). Although nitrilases have been well studied, the nitrilase obtained in this study is quite different compared with the previously reported nitrilases from different origins (Table 1) which share the same conserved regions, including PGYP (residues 52−55), RRKLKPTHVER (residues 128−138), CWEH (residues 164−167), and GHYS (residues 295−298) (Figure 1).

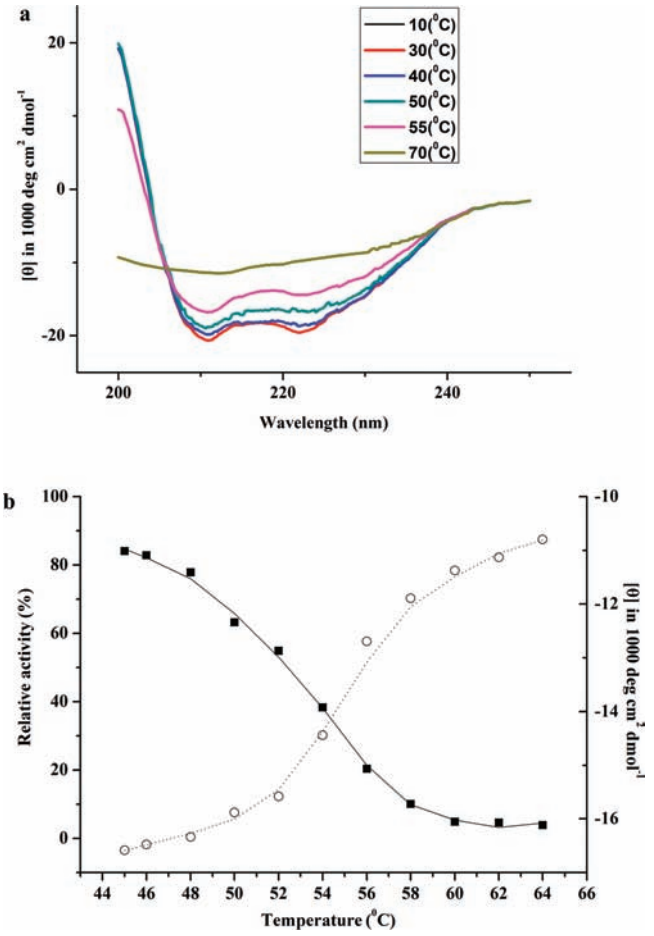

Figure 4. Spectroscopic structural analysis and thermal stability of nitrilase. (a) CD wavelength scans of nitrilase at pH 7.5. The data are represented as the average of three trials. (b) Far-UV CD spectra of nitrilase from 44 °C to 64 °C. Relative activity and molar ellipticity were measured at 222 nm.

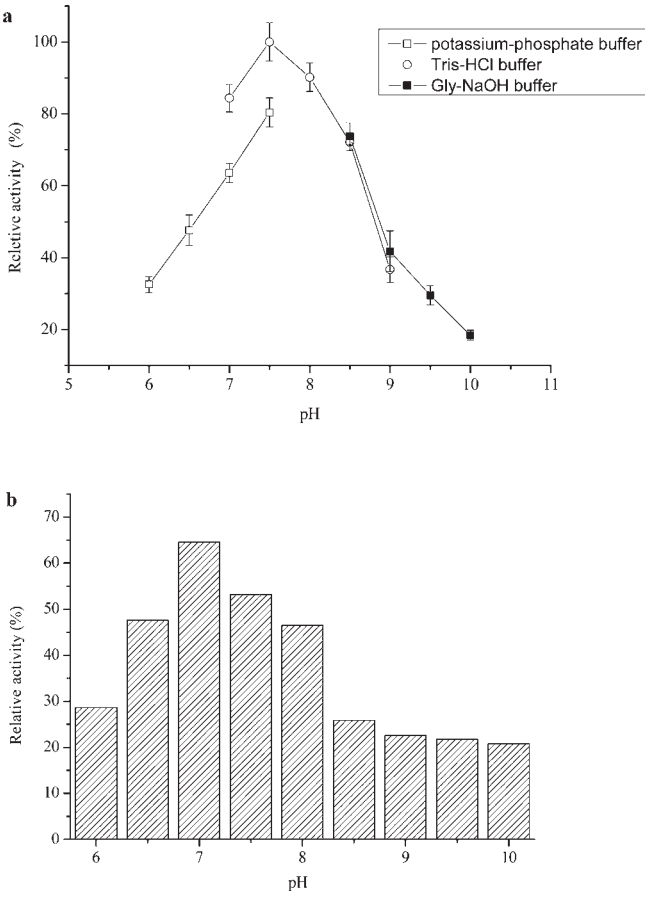

Figure 5. Effect of pH on activity of nitrilase and stability. (a) Effect of pH on activity of nitrilase. Reactions were performed at 40 °C, 150 rpm, for 10 min with different buffers. (b) pH stability: The purified enzyme was incubated in different buffers at pHs ranging from 6.0 to 10.0 for 1 h, and the residual activity was tested. All experiments were performed in triplicate.

Expression of the Nitrilase Gene and Its Purification. To express the gene encoding nitrilase, primers P3 and P4 were designed according to the sequencing result of pMD18-T-NIT, with *Bam*HI and *Sal*I sites, respectively. PCR amplification was conducted by adopting the recombined plasmid pMD18-T-NIT obtained above as the template, and the DNA fragment encoding the nitrilase gene was subcloned into an expression vector pET28b(+) to construct the recombinant plasmid pET28b(+)-NIT. Subsequently, the recombinant plasmids were then introduced into competent cells of *E. coli* BL21(DE3), and many clones were picked up. The positive transformant containing recombinant pET28b(+)-NIT was identified by colony PCR and double enzymatic digestion. The recombinant cell harboring pET28b(+)-NIT was induced by 0.1 mM of IPTG at 28 °C for about 20 h when the OD_{600} reached the value of 0.6. Protein bands from SDS-PAGE were visualized by staining with Coomassie brilliant blue. The thick protein band corresponding to the subunit of nitrilase with the 6×His-tag shows an apparent molecular mass of about 44 kDa (Figure 2). These data are in excellent agreement with those derived from DNA sequencing. The purified protein was observed as a single band with SDS-PAGE (Figure 2), indicating that the protein was quite pure.

Optimal Temperature and Thermostability. To evaluate the optimal temperature of the enzyme, activities were assayed at various temperatures ranging from 25 °C to 65 °C using standard assay conditions, and detailed results are shown in Figure 3a. The activity of nitrilase increased from 25 °C to 40 °C and reached its maximum at a temperature of 40 °C which is similar to that of nitrilase from *P. putida*.[43] However, after this apex point, the activity of nitrilase decreased sharply and the activity was totally lost at 65 °C. To investigate the thermostatbility of nitrilase, the enzyme was incubated at different temperatures ranging from 35 °C to 65 °C, and the activities of enzymes that were assayed under the standard reaction conditions were used as control. The activity decreased markedly above 55 °C, which might be explained by the inactivation or changes in configuration of the nitrilase while, like most of the nitrilases reported in literature, the enzyme was labile at higher temperature as revealed by a half-life of 57 min at 40 °C, 42 min at 45 °C, and 20 min at 55 °C, respectively (Figure 3b). The enzyme thermostability was better than that of nitrilase from *P. putida*, reported to have half-lives of 76 min at 40 °C and 9 min at 50 °C, respectively.[43] Indeed, the enzyme seemed to be still sensitive to heat, which can be corroborated by thermostability measurements with CD (Figure 4) that *A. faecalis* nitrilase exhibited a melting temperature of 56 °C.[44]

Table 2. Effect of Metal Ions and Some Chemicals on the Activity of Nitrilase from *A. faecalis* ZJUTB10[a]

reagent (5 mM)	relative activity (%)
control	100
$CuCl_2$	16
$CoCl_2$	20
$FeCl_3$	81
$FeCl_2$	83
$NiCl_2$	17
$MnCl_2$	78
$CaCl_2$	102
LiCl	89
$MgCl_2$	122
$BaCl_2$	92
$ZnSO_4$	64
$AgNO_3$	6
$HgCl_2$	0
$EDTA-Na_2$	96

[a] Enzyme activities were determined under standard assay conditions, in the presence of 5 mM of each salt and expressed as the percentage with respect to the activity of a control reaction carried out in the absence of any salt.

Optimal pH and pH Stability. To investigate the optimal pH, buffers including potassium phosphate buffer (pH 6.0−7.5), Tris-HCl buffer (pH 7.0−9.0), and Gly-NaOH buffer (pH 8.5−10.0) with 50 mM for each were used. The results showed that the highest activity was observed in Tris-HCl at pH 7.5 though nitrilase functions in all the buffers (Figure 5a). The pH stability of enzyme was examined by assaying the residual activity under the standard assay conditions after incubation. The results shown in Figure 5b suggested that the nitrilase was more stable at pH 7.0 with about 65% residual activity. However, higher pH (pH > 8.0) resulted in significant reduction in the residual activity to approximately 20% (Figure 5b).

Effects of Metal Ions and Ethylenediaminetetraacetic Acid (EDTA). The effects of different metal ions and EDTA on the activity of nitrilase were examined by incubating the enzyme in the presence of the reagents. The activity assayed in the absence of metal ions and EDTA was considered as the control. The data shown in Table 2 indicate that activity of nitrilase was affected by most tested metal ions and was especially strongly inhibited by Cu^{2+}, Co^{2+}, Ni^{2+}, Ag^{+}, and Hg^{2+}. As we know, Ag^{+} and Hg^{2+} have strong binding to sulfhydryl reagents, which indicates that the thiol group is essential for the catalytic activity. In addition, the results of metal ions analysis showed that the Mg^{2+} could slightly activate the activity of nitrilase. However, no inhibition was observed in the presence of chelating agent EDTA, indicating that this nitrilase had no metal ion requirements.

Time Course of Mandelonitrile Hydrolysis with Recombinant Nitrilase. The data shown in Figure 6 indicate that the *R*-isomer was rapidly transformed to acid, which was much faster than that for the *S*-counterpart. After 35 min, the concentration of (*R*)-(−)-mandelic acid in the reaction mixture reached approximately 20 mM by adding 1 mg of purified enzyme in 10 mL of Tris-HCl buffer at pH 7.5. Because of the efficient in situ racemization of the unreacted (*S*)-mandelonitrile at slightly alkaline pH,[37] we did not detect any amount of mandelamide as a possible byproduct, resulting in a substrate

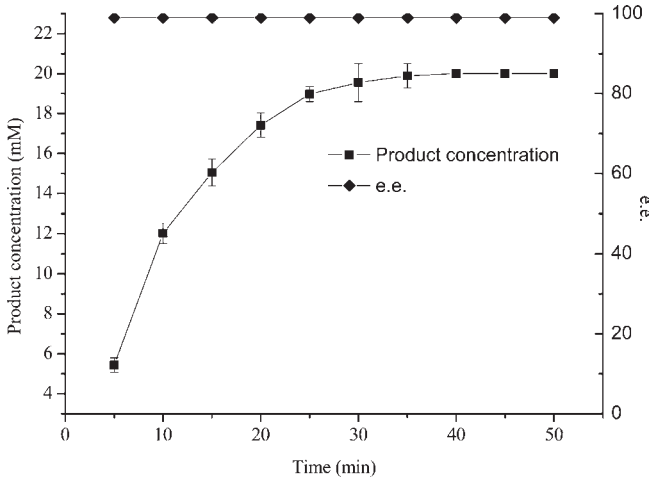

Figure 6. Time course of mandelonitrile by the nitrilase. Reactions were performed at 40 °C, 150 rpm. The purified enzyme (1 mg) was incubated with 10 mL of 50 mM Tris-HCl buffer (pH 7.5) and 20 mM for each nitrile.

conversion rate of 100%. However, the nitrilase of *P. fluorescens* EBC191 only produced 19% of the total products in terms of the corresponding acid.[45] These results indicate that a complicated and costly downstream process can be avoided and that a high concentration and purity of product can be attained, thus reducing the operation cost of an enzymatic process from the viewpoint of industrial application. The optical purity of the (*R*)-(−)-mandelic acid product was maintained above 99% ee during the reaction process (Figure 6), which was the same as that from using the strain *A. faecalis* ZJUTB10 as catalyst (>99% ee).[16]

Determination of the Kinetic Parameters. For determining the kinetics of the hydrolysis reaction, the rate of this reaction was determined at different concentrations [S] (0−60 mM) of racemic mandelonitrile (Figure 7). The experimental data collected were fitted to the Michalis−Menten equation ($v_0 = (v_{max}[S]/2)/(k_m + [S]/2)$) to determine the K_m and v_{max}. The K_m and v_{max} of the nitrilase for (*R*)-(−)-mandelic acid were calculated to be 4.74 mM and 15.85 μmol min^{-1} mg^{-1}, respectively.

Substrate Specificity. The nitrilase from *A. faecalis* ZJUTB10 was assessed for hydrolytic activity on a set of nitriles listed in Table 3. The purified enzyme has no activity toward aminobutytonitrile, 2,2-dimethylcyclopropyl cyanide, and 2-amino-2, 3-dimethylbutanenitrile, very low activity toward 4-aminobenzonitrile and iminodiacetonitrile, but high activity toward phenylacetonitrile, *o*-methoxyphenylacetic acid, *m*-methoxyphenylacetic acid, and *p*-methoxyphenylacetic acid. From the substrate specificity study, though the enzyme exhibited activity toward both classes of aromatic and arylacetonitriles, we found that the nitrilase showed higher activity toward the arylacetonitriles, which further confirmed that *A. faecalis* nitrilase obtained here belongs to the arylacetonitrilase family.

Homology Modeling and Docking. The three-dimensional homology models of nitrilases were generated using Build Homology Models (MODELER) module in Discovery Studio 2.1 (Accelrys Software). The crystal structure of hypothetical protein PH0642 (PDB accession code 1J31, resolution 1.6 Å) from *Pyrococcus horikoshii*,[46] and a thermoactive nitrilase PaNit (PDB accession code 3IVZ, resolution 1.57 Å) from *P. abyssi*,[47]

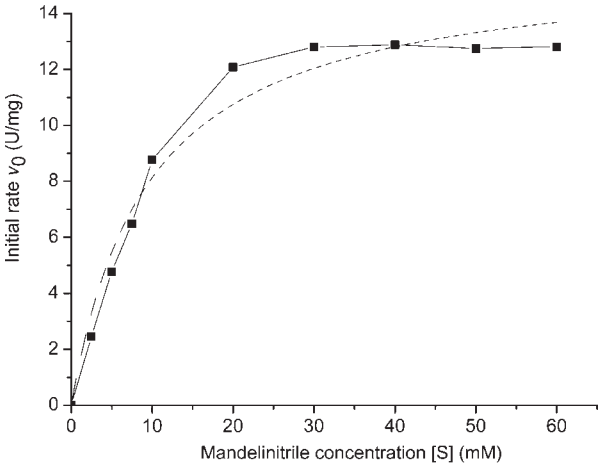

Figure 7. Reaction rate at different mandelonitrile concentrations. Reactions were performed for 10 min at 40 °C, 150 rpm, with 50 mM Tris-HCl buffer (pH 7.5): (···) fitting curve, (—) experimental curve.

Table 3. Substrate Specificity of the Nitrilase[a]

substrate	relative activity (%)	docked energy (kcal/mol)
(*R*)-mandelonitrile	100	−2.664
iminodiacetonitrile	12	−2.473
acetonitrile	36	−2.488
aminobutyronitrile	0	−1.783
adiponitrile	76	−2.434
glycolonitrile	24	−1.966
4-aminobenzonitrile	16	−1.880
2,2-dimethylcyclopropyl cyanide	2	−1.875
2-amino-2,3-dimethylbutanenitrile	0	−1.691
benzonitrile	162	−2.244
o-methoxyphenylacetonitrile	153	−2.239
m-methoxyphenylacetonitrile	210	−2.576
p-methoxyphenylacetonitrile	146	−1.676
phenylacetonitrile	263	−2.800
acrylonitrile	53	−2.357

[a] Activity of nitrilase was assayed under the standard assay conditions with 20 mM substrate. The activity with mandelonitrile was set as 100%.

were used as templates. A BLAST search of the Protein Data Bank demonstrated the strongest similarity between the nitrilase from *A. faecalis* ZJUTB10 and the protein PH0642 (PDB 1J31)/PaNit (PDB 3IVZ) belonging to the nitrilase superfamily. Comparative modeling was used to generate the most probable structure of the query protein by the alignment with template sequences, simultaneously satisfying spatial restraints and local molecular geometry. Sequence identity between target and templates were around 23% according to PDB, respectively. Despite varying sequence identity, all nitrilase structures share a characteristic monomer fold and contain glutamate, lysine, and cysteine in their catalytic sites. The discrete optimized protein energy score in MODELER was also calculated to determine the quality of protein structures. The generated structure was

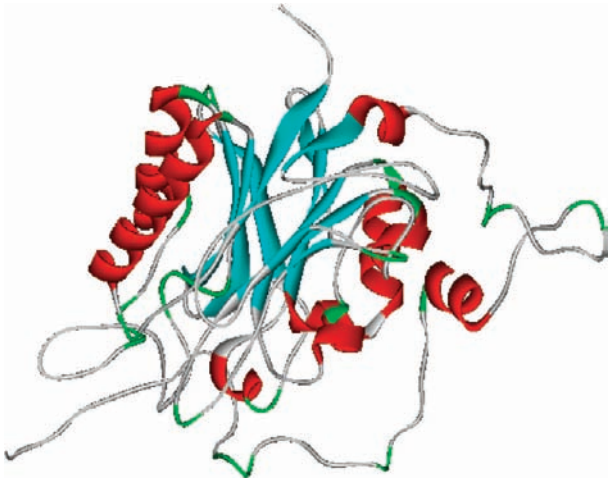

Figure 8. View of modeled structure of *A. faecalis* ZJUTB10 nitrilase.

improved by subsequent refinement of the loop conformations by assessing the compatibility of an amino acid sequence to known PDB structures using the Protein Health module in DS 2.1. The geometry of loop regions was corrected using Refine Loop/MODELER. Finally, the best quality model (Figure 8) was chosen for further calculations, molecular modeling, and docking studies. The conserved catalytic residues Glu-47, Lys-129, and Cys-163 from nitrilase protein were proposed to be the catalytic triad of nitrilase and have similar orientations and locations in the nitrilase model. To verify the prediction of the conserved catalytic residues, and test whether the predicted conserved catalytic residues play a role in catalysis, these residues were mutated by site-directed mutagenesis. The mutations of these residues resulted in inactivated enzymes, the activities being hardly detectable, indicating that these residues are involved in enzymatic activity. However, the accuracy of the model is limited, as it is based on homology modeling and not on a crystal structure. To confirm our molecular modeling and structural analysis, the crystal structure of *A. faecalis* ZJUTB10 nitrilase should be determined.

The molecular docking studies of the *A. faecalis* ZJUTB10 nitrilase show substrate interactions in the active site. The resulting model was used for further docking studies. Hydrogen atoms were added to the protein model. The added hydrogen atoms were minimized to have a stable energy conformation and also to relax the conformation from close contacts. The active site of nitrilase was defined, and a cubic of 40 $Å^3$ was generated around the catalytic triad pocket (CEK). With the AD4 force field, 53 substrates (Table 4) were able to be docked in the receptors (enzymes) in productive conformations. The docked energy (10 docked conformations) of each substrate/enzyme pair was compared, and the results are shown in Table 3. In the catalytic triad, Cys-163 attacks the cyano group of the nitriles as a nucleophile, Glu-47 assumes the role of a general base, and Lys-129 is involved in the stabilization of a tetrahedral intermediate structure, which are the same features as those observed for the nitrilase from *P. fluorescens* Pf-5.[48]

The docking results (Table 4) indicated that nitrilase obtained in this study could hydrolyze arylacetonitriles and aromatic nitriles in the following preference: meta > ortho > para. However, this nitrilase has no activity toward aliphatic nitriles with long chains and nitriles with an amino group, which has

Table 4. Substrates Docking Studies

substrate	molecular weight	docked energy (kcal/mol)	substrate	molecular weight	docked energy (kcal/mol)
benzonitrile	103.12	−2.244	mandelonitrile	133.15	−2.664
1,2-benzodinitrile	128.13	−2.239	*o*-methoxyphenylacetonitrile	147.18	−2.239
1,3-benzodinitrile	128.13	−2.538	*m*-methoxyphenylacetonitrile	147.18	−2.576
1,4-benzodinitrile	128.13	−2.119	*p*-methoxyphenylacetonitrile	147.18	−1.676
2-fluorobenzonitrile	121.11	−1.568	*p*-fluorobenzylcyanide	135.14	−1.696
3-fluorobenzonitrile	121.11	−2.146	*p*-nitrobenzylcyanide	162.15	−1.214
4-fluorobenzonitrile	121.11	−2.151	*p*-aminobenzylcyanide	132.16	−1.601
2-chlorobenzonitrile	137.57	−2.261	propionitrile	55.08	−2.230
3-chlorobenzonitrile	137.57	−2.564	acrylonitrile	72.06	−2.357
4-chlorobenzonitrile	137.57	−2.363	butyronitrile	69.11	−2.534
2-bromobenzonitrile	182.02	−2.320	isobutyronitrile	69.11	−2.652
3-bromobenzonitrile	182.02	−2.584	adiponitrile	108.14	−2.434
4-bromobenzonitrile	182.02	−2.122	glutaronitrile	94.12	−2.665
2-nitrobenzonitrile	148.12	−0.462	succinonitrile	80.09	−2.670
3-nitrobenzonitrile	148.12	−1.593	sebaconitrile	164.25	7.410
4-nitrobenzonitrile	148.12	−1.233	methacrylonitrile	67.09	−2.591
2-aminobenzonitrile	118.14	−1.630	aminoacetonitrile	56.07	−1.896
3-aminobenzonitrile	118.14	−1.962	aminobutyronitrile	84.12	−1.783
4-aminobenzonitrile	118.14	−1.880	glycolonitrile	57.05	−1.966
2-hydroxybenzonitrile	119.12	−2.085	iminodiacetonitrile	95.10	−2.473
3-hydroxybenzonitrile	119.12	−2.420	2-furanocarbonitrile	93.08	−2.492
4-hydroxybenzonitrile	119.12	−2.288	2-pyridinacetonitrile	209.25	−2.547
o-tolunitrile	117.15	−2.223	3-pyridinacetonitrile	209.25	−2.515
m-tolunitrile	117.15	−2.603	2-cyanopyridine	104.11	−2.369
p-tolunitrile	117.15	−2.423	3-cyanopyridine	104.11	−2.548
3-phenylpropionitrile	131.17	−1.524	4-cyanopyridine	104.11	−2.137
phenylacetonitrile	117.15	−2.800			

been confirmed by the data listed in Table 3. The results of docking also showed that this enzyme belongs to the arylacetonitrilase family. Structure determination of the enzyme−substrate complexes is needed to provide further evidence for this conclusion.

DISCUSSION

Nitrilases are important to many organisms because of their ability to convert chemically reactive and harmful nitriles into carboxylic acids as the sole product under mild conditions. As promising biocatalysts, in recent years, nitrilases also have been widely used in industrial applications for the preparation of pharmaceuticals and other fine chemicals under mild conditions. Because of the importance of nitrilases in industrial applications, screening, and exploitation, development of new nitrilases has recently received considerable attention. In this study, a new *A. faecalis* nitrilase was obtained and cloned into *E. coli* cells. Characterization of the recombinant enzyme showed that this nitrilase has very excellent activity toward (*R*)-mandelonitrile and other sets of nitriles. Especially, the nitrilase from *A. faecalis* ZJUTB10 has a preference for arylacetonitriles. This study further confirmed that none of the nitrilases show identical properties. The most notable differences between the enzymes are in substrate specificity, native structure and aggregation properties, and pH optima.[14]

There are several factors that influence the function of *A. faecalis* ZJUTB10 nitrilase. From this study, we found that this nitrilase was more stable to heat compared to other nitrilases,[38,43] and neutral pH favored its activity. Though several reports have demonstrated that most nitrilases are ion-independent,[27,28] *A. faecalis* ZJUTB10 nitrilase was enhanced by Mg^{2+}; thus, the relationship and function of Mg^{2+} with the nitrilase obtained in this study need further investigation.

Modeling and mutation studies showed that conserved catalytic residues Cys-163, Glu-47, and Lys-129 are the catalytic triad of the nitrilase obtained in this study, and these residues are essential in the activity of nitrilase. According to reports[6,44] and on the basis of the structural assignment, a section-conserved sequence (residues 164−167 CEEH) was found in the substrate binding pocket and is very close to the active site Cys163. The 'enantioselective hot spot' amino acids around 190 are situated in the loop between α6 (α4 in the *A. faecallis* nitrilase) and β8. These regions would be attractive targets for exploring higher selectivity and activity of nitrilase in further studies using the molecular modification of proteins.[49]

When a substrate molecule diffuses into the pocket, it can bind onto the CEK of nitrilase in an orthogonal orientation (Figure 9a). Glu-47 may further mediate the proton transfer from the SH group of Cys-163, resulting in a strongly nucleophilic S ion to initiate the first attack on the cyano carbon atom of the substrate. In the CEK, cysteine attacks the cyano group of the nitrile as a nucleophile, glutamate acts as a general base, and lysine is involved in stabilization of the tetrahedral intermediate.[47] When (*R*)-mandelonitrile was docked in the active site of nitrilase (Figure 9b), a hydrogen bond (bond length 3.5 Å) was observed between the N (cyano nitrogen) of mandelonitrile

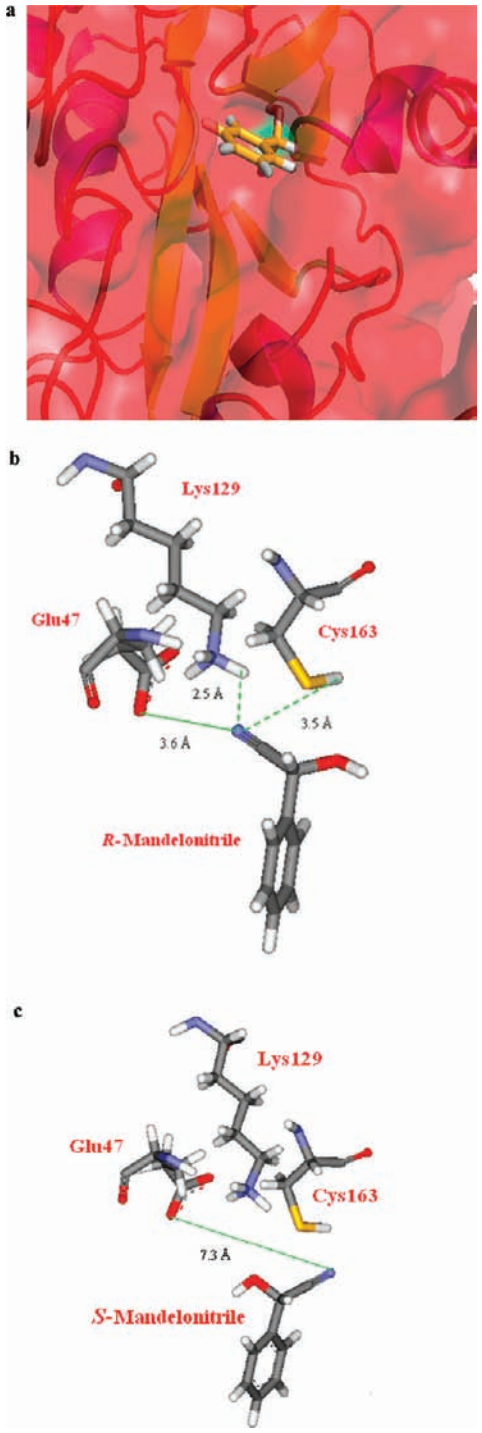

Figure 9. A stereoview of the putative intermediate. (a) Mandelonitrile docking into the active site of nitrilase. (b) Catalytic triad of nitrilase with (*R*)-mandelonitrile. (c) Catalytic triad of nitrilase with (*S*)-mandelonitrile.

and the H associated with the sulfur of Cys-163. Similarly, a second hydrogen bond (2.5 Å) was observed between the N of mandelonitrile and Lys-129, resulting in a stable transition state intermediate and proper orientation for nucleophilic attack on the first cyano carbon by the SH group of Cys-163. However, when (*S*)-mandelonitrile was used as a substrate to dock into the catalytic active triad, the distance between Glu-47 and the CN group on (*S*)-mandelonitrile is 7.3 Å because its position is hindered. This distance is beyond of the maximum catalytic distance for this *R*-selective nitrilase (Figure 9c). Docked energies for (*R*)-mandelonitrile (−2.664 kcal/mol) and (*S*)-mandelonitrile (−2.013 kcal/mol) further confirmed that nitrilase in this study can selectively catalyze (*R*)-mandelonitrile to (*R*)-mandelic acid. Analysis of catalytic characteristics based on structure modeling and molecular docking will provide new insight into nitrilase and help to clarify the fundamentals for its application. To confirm our molecular modeling and structural analysis, the crystal structure of nitrilase should be determined, which is in progress in our laboratory.

AUTHOR INFORMATION

Corresponding Author

*Tel: +86-571-88320614. Fax: +86-571-88320630. E-mail: zhengyg@zjut.edu.cn.

Funding Sources

†The authors gratefully acknowledge the financial support of the National High Technology Research and Development Program of China (863 Program) (No. 2009AA02Z203), the Major Basic Research Development Program of China (973 Project) (No. 2009CB724704), National Natural Science Foundation of China (No. 31170761), Natural Science Foundation of Zhejiang Province (No. Z4090612, Y4110409 and No. R3110155), and Qianjiang Talent Project of Zhejiang Province.

REFERENCES

(1) Lynd, L. R.; Wyman, C. E.; Gerngross, T. U. Biocommodity engineering. *Biotechnol. Prog.* **1999**, *15* (5), 777–793.

(2) Feng, X. W.; Li, C.; Wang, N.; Li, K.; Zhang, W. W.; Wang, Z.; Yu, X. Q. Lipase-catalysed decarboxylative aldol reaction and decarboxylative Knoevenagel reaction. *Green Chem.* **2009**, *11* (12), 1933–1936.

(3) Guebitz, G. M.; Cavaco-Paulo, A. Enzymes go big: surface hydrolysis and functionalisation of synthetic polymers. *Trends Biotechnol.* **2008**, *26* (1), 32–38.

(4) Nagasawa, T.; Yamada, H. Microbial transformations of nitriles. *Trends Biotechnol.* **1989**, *7* (6), 153–158.

(5) Kobayashi, M.; Shimizu, S. Nitrile hydrolases. *Curr. Opin. Chem. Biol.* **2000**, *4* (1), 95–102.

(6) Thuku, R. N.; Brady, D.; Benedik, M. J.; Sewell, B. T. Microbial nitrilases: versatile, spiral forming, industrial enzymes. *J. Appl. Microbiol.* **2009**, *106* (3), 703–727.

(7) Jandhyala, D. M.; Willson, R. C.; Sewell, B. T.; Benedik, M. J. Comparison of cyanide-degrading nitrilases. *Appl. Microbiol. Biotechnol.* **2005**, *68* (3), 327–335.

(8) Zheng, Y. G.; Chen, J.; Liu, Z. Q.; Wu, M. H.; Xing, L. Y.; Shen, Y. C. Isolation, identification and characterization of *Bacillus subtilis* ZJB-063, a versatile nitrile-converting bacterium. *Appl. Microbiol. Biotechnol.* **2008**, *77* (5), 985–993.

(9) Liu, Z. Q.; Li, F. F.; Cheng, F.; Zhang, T.; You, Z. Y.; Xu, J. M.; Xue, Y. P.; Zheng, Y. G.; Shen, Y. C. A Novel synthesis of iminodiacetic acid: Biocatalysis by whole *Alcaligenes faecalis* ZJB-09133 cells from iminodiacetonitrile. *Biotechnol. Prog.* **2011**, *27* (3), 698–705.

(10) Fernandes, B. C. M.; Mateo, C.; Kiziak, C.; Chmura, A.; Wacker, J.; van Rantwijk, F.; Stolz, A.; Sheldon, R. A. Nitrile hydratase activity of a recombinant nitrilase. *Adv. Synth. Catal.* **2006**, *348* (18), 2597–2603.

(11) .Pace, H. C.; Brenner, C. The nitrilase superfamily: classification, structure and function. *Genome Biol.* **2001**, *2* (1), REVIEWS0001.1−0001.9.

(12) Banerjee, A.; Sharma, R.; Banerjee, U. C. The nitrile-degrading enzymes: current status and future prospects. *Appl. Microbiol. Biotechnol.* **2002**, *60* (1−2), 33–44.

(13) Brenner, C. Catalysis in the nitrilase superfamily. *Curr. Opin. Struct. Biol.* **2002**, *12* (6), 775–782.

(14) O'Reilly, C.; Turner, P. D. The nitrilase family of CN hydrolysing enzymes - a comparative study. *J. Appl. Microbiol.* **2003**, *95* (6), 1161–1174.

(15) Williamson, D. S.; Dent, K. C.; Weber, B. W.; Varsani, A.; Frederick, J.; Thuku, R. N.; Cameron, R. A.; van Heerden, J. H.; Cowan, D. A.; Sewell, B. T. Structural and biochemical characterization of a nitrilase from the thermophilic bacterium, *Geobacillus pallidus* RAPc8. *Appl. Microbiol. Biotechnol.* **2010**, *88* (1), 143–153.

(16) Xue, Y. P.; Xu, S. Z.; Liu, Z. Q.; Zheng, Y. G.; Shen, Y. C. Enantioselective biocatalytic hydrolysis of (*R*,*S*)-mandelonitrile for production of (*R*)-(−)-mandelic acid by a newly isolated mutant strain. *J. Ind. Microbiol. Biotechnol.* **2011**, *38* (2), 337–345.

(17) Sambrook, J.; Russell, D. W. Molecular cloning: A laboratory manual. In *Molecular cloning: A laboratory manual*; Cold Spring Harbor Laboratory Press: Woodbury, NY, 2001.

(18) Laemmli, U. K. Cleavage of structural proteins during the assembly of the head of bacteriophage T4. *Nature* **1970**, *227* (5259), 680–685.

(19) Bradford, M. M. A rapid and sensitive method for the quantitation of microgram quantities of protein utilizing the principle of protein-dye binding. *Anal. Biochem.* **1976**, *72*, 248–254.

(20) Fasman, G. D. *Circular Dichroism and the Conformational Analysis of Biomolecules*; Plenum Press: New York, 1996.

(21) Liu, Z. Q.; Gosser, Y.; Baker, P. J.; Ravee, Y.; Lu, Z. Y.; Alemu, G.; Li, H. G.; Butterfoss, G. L.; Kong, X. P.; Gross, R.; Montclare, J. K. Structural and functional studies of *Aspergillus oryzae* cutinase: Enhanced thermostability and hydrolytic activity of synthetic ester and polyester degradation. *J. Am. Chem. Soc.* **2009**, *131* (43), 15711–15716.

(22) Greenfield, N. J. Using circular dichroism spectra to estimate protein secondary structure. *Nat. Protoc.* **2006**, *1* (6), 2876–2890.

(23) Pace, C. N.; Grimsley, G. R.; Thomson, J. A.; Barnett, B. J. Conformational stability and activity of ribonuclease T1 with zero, one, and two intact disulfide bonds. *J. Biol. Chem.* **1988**, *263* (24), 11820–11825.

(24) Morris, G. M.; Goodsell, D. S.; Halliday, R. S.; Huey, R.; Hart, W. E.; Belew, R. K.; Olson, A. J. Automated docking using a Lamarckian genetic algorithm and an empirical binding free energy function. *J. Comput. Chem.* **1998**, *19* (14), 1639–1662.

(25) Thompson, J. D.; Gibson, T. J.; Plewniak, F.; Jeanmougin, F.; Higgins, D. G. The CLUSTAL_X windows interface: flexible strategies for multiple sequence alignment aided by quality analysis tools. *Nucleic Acids Res.* **1997**, *25* (24), 4876–4882.

(26) Gouet, P.; Courcelle, E.; Stuart, D. I.; Metoz, F. ESPript: analysis of multiple sequence alignments in PostScript. *Bioinformatics* **1999**, *15* (4), 305–308.

(27) Kaplan, O.; Vejvoda, V.; Plihal, O.; Pompach, P.; Kavan, D.; Bojarova, P.; Bezouska, K.; Mackova, M.; Cantarella, M.; Jirku, V.; Kren, V.; Martinkova, L. Purification and characterization of a nitrilase from *Aspergillus niger* K10. *Appl. Microbiol. Biotechnol.* **2006**, *73* (3), 567–575.

(28) Almatawah, Q. A.; Cramp, R.; Cowan, D. A. Characterization of an inducible nitrilase from a thermophilic bacillus. *Extremophiles* **1999**, *3* (4), 283–291.

(29) Harper, D. B. Microbial metabolism of aromatic nitriles. Enzymology of C-N cleavage by *Nocardia* sp. (*Rhodochrous* group) N.C.I.B. 11216. *Biochem. J.* **1977**, *165* (2), 309–319.

(30) Hoyle, A. J.; Bunch, A. W.; Knowles, C. J. The nitrilases of *Rhodococcus rhodochrous* NCIMB 11216. *Enzyme Microb. Technol.* **1998**, *23* (7−8), 475–482.

(31) Kobayashi, M.; Nagasawa, T.; Yamada, H. Nitrilase of *Rhodococcus rhodochrous* J1. Purification and characterization. *Eur. J. Biochem.* **1989**, *182* (2), 349–356.

(32) Nagasawa, T.; Wieser, M.; Nakamura, T.; Iwahara, N.; Yoshida, T.; Gekko, K. Nitrilase of *Rhodococcus rhodochrous* J1 - Conversion into the active form by subunit association. *Eur. J. Biochem.* **2000**, *267* (1), 138–144.

(33) Gavagan, J. E.; DiCosimo, R.; Eisenberg, A.; Fager, S. K.; Folsom, P. W.; Hann, E. C.; Schneider, K. J.; Fallon, R. D. A Gram-negative bacterium producing a heat-stable nitrilase highly active on aliphatic dinitriles. *Appl. Microbiol. Biotechnol.* **1999**, *52* (5), 654–659.

(34) Chauhan, S.; Wu, S.; Blumerman, S.; Fallon, R. D.; Gavagan, J. E.; DiCosimo, R.; Payne, M. S. Purification, cloning, sequencing and over-expression in *Escherichia coli* of a regioselective aliphatic nitrilase from *Acidovorax facilis* 72W. *Appl. Microbiol. Biotechnol.* **2003**, *61* (2), 118–122.

(35) Zhu, D. M.; Mukherjee, C.; Yang, Y.; Rios, B. E.; Gallagher, D. T.; Smith, N. N.; Biehl, E. R.; Hua, L. A new nitrilase from *Bradyrhizobium japonicum* USDA 110 - Gene cloning, biochemical characterization and substrate specificity. *J. Biotechnol.* **2008**, *133* (3), 327–333.

(36) Kobayashi, M.; Yanaka, N.; Nagasawa, T.; Yamada, H. Purification and Characterization of a Novel Nitrilase of *Rhodococcus-Rhodochrous* K22 That Acts on Aliphatic Nitriles. *J. Bacteriol.* **1990**, *172* (9), 4807–4815.

(37) Yamamoto, K.; Oishi, K.; Fujimatsu, I.; Komatsu, K. I. Production of *R*-(−)-Mandelic Acid from Mandelonitrile by *Alcaligenes-Faecalis* Atcc-8750. *Appl. Environ. Microbiol.* **1991**, *57* (10), 3028–3032.

(38) Nagasawa, T.; Mauger, J.; Yamada, H. A Novel Nitrilase, Arylacetonitrilase, of *Alcaligenes-Faecalis* Jm3 - Purification and Characterization. *Eur. J. Biochem.* **1990**, *194* (3), 765–772.

(39) Kobayashi, M.; Izui, H.; Nagasawa, T.; Yamada, H. Nitrilase in biosynthesis of the plant hormone indole-3-acetic-acid from indole-3-acetonitrile - cloning of the *Alcaligenes* gene and site-directed mutagenesis of cysteine residues. *Proc. Natl. Acad. Sci. U.S.A.* **1993**, *90* (1), 247–251.

(40) Zhu, D. M.; Mukherjee, C.; Biehl, E. R.; Hua, L. Discovery of a mandelonitrile hydrolase from *Bradyrhizobium japonicum* USDA110 by rational genome mining. *J. Biotechnol.* **2007**, *129* (4), 645–650.

(41) Watanabe, A.; Yano, K.; Ikebukuro, K.; Karube, I. Cloning and expression of a gene encoding cyanidase from *Pseudomonas stutzeri* AK61. *Appl. Microbiol. Biotechnol.* **1998**, *50* (1), 93–97.

(42) Barclay, M.; Day, J. C.; Thompson, I. P.; Knowles, C. J.; Bailey, M. J. Substrate-regulated cyanide hydratase (chy) gene expression in *Fusarium solani*: the potential of a transcription-based assay for monitoring the biotransformation of cyanide complexes. *Environ. Microbiol.* **2002**, *4* (3), 183–189.

(43) Banerjee, A.; Kaul, P.; Banerjee, U. C. Purification and characterization of an enantioselective arylacetonitrilase from *Pseudomonas putida*. *Arch. Microbiol.* **2006**, *184* (6), 407–418.

(44) DeSantis, G.; Wong, K.; Farwell, B.; Chatman, K.; Zhu, Z. L.; Tomlinson, G.; Huang, H. J.; Tan, X. Q.; Bibbs, L.; Chen, P.; Kretz, K.; Burk, M. J. Creation of a productive, highly enantioselective nitrilase through gene site saturation mutagenesis (GSSM). *J. Am. Chem. Soc.* **2003**, *125* (38), 11476–11477.

(45) Kiziak, C.; Conradt, D.; Stolz, A.; Mattes, R.; Klein, J. Nitrilase from *Pseudomonas fluorescens* EBC191: cloning and heterologous expression of the gene and biochemical characterization of the recombinant enzyme. *Microbiology* **2005**, *151*, 3639–3648.

(46) Sakai, N.; Tajika, Y.; Yao, M.; Watanabe, N.; Tanaka, I. Crystal structure of hypothetical protein PH0642 from *Pyrococcus horikoshii* at 1.6 angstrom resolution. *Proteins* **2004**, *57* (4), 869–873.

(47) Rypniewski, W.; Raczynska, J. E.; Vorgias, C. E.; Antranikian, G. Crystallographic analysis of a thermoactive nitrilase. *J. Struct. Biol.* **2011**, *173* (2), 294–302.

(48) Kim, J. S.; Tiwari, M. K.; Moon, H. J.; Jeya, M.; Ramu, T.; Oh, D. K.; Kim, I. W.; Lee, J. K. Identification and characterization of a novel nitrilase from *Pseudomonas fluorescens* Pf-5. *Appl. Microbiol. Biotechnol.* **2009**, *83* (2), 273–283.

(49) Liu, Z. Q.; Leng, Y.; Sun, Z. H. Directed evolution and characterization of a novel D-pantonohydrolase from *Fusarium moniliforme*. *J. Agric. Food Chem.* **2006**, *54* (16), 5823–5830.